JOURNAL OF PHYSICAL ORGANIC CHEMISTRY, VOL. 8, 659–670 (1995)

# MOLECULAR AGGREGATES BETWEEN OCTAETHYLTETRATHIAPORPHYRIN DICATION ($OTP^{2+}$) AND OCTAETHYLPORPHYRIN ($H_2OEP$) AND ITS METAL COMPLEXES

ATIF MAHAMMED, MORDECAI RABINOVITZ, ROY E. HOFFMAN AND ITAMAR WILLNER*
*Hebrew University of Jerusalem, Jerusalem 91904, Israel*

AND

EMANUEL VOGEL AND MICHAEL POHL
*Institut für Organische Chemie der Universität Köln, D-50939 Cologne, Germany*

**The octaethyltetrathiaporphyrin dication, $OTP^{2+}$, forms 1:1 intermolecular donor–acceptor complexes with $Ni^{II}$-, $V^{IV}O$- and $Fe^{III}$-octaethylporphyrins. The association constants of the complexes are governed by the oxidation potential of the metallo-octaethylporphyrins and by secondary electrostatic interactions. Octaethylporphyrin, $H_2OEP$, forms intermolecular complexes with $OTP^{2+}$. Kinetic analyses of the formation of the various complexes revealed the formation of a primary complex exhibiting the stoichiometry $(OTP^{2+})_2(H_2OEP)$. This intermolecular complex transforms into a thermodynamically stabilized intermolecular assembly with a stoichiometry corresponding to $(OTP^{2+})_4H_2OEP$. The activation barrier associated with the conversion of the primary complex to the thermodynamically stabilized assembly is $E_a = 16{\cdot}5$ kcal mol$^{-1}$ (1 kcal = 4·184 kJ). The association constant of the complex $(OTP^{2+})_2(H_2OEP)$ is $K_1 = 1{\cdot}3 \times 10^{10}$ M$^{-2}$ and the equilibrium constant between the two coexisting intermolecular complexes $(OTP^{2+})_4(H_2OEP)$ and $(OTP^{2+})_2(H_2OEP)$ is $K_2 = 7{\cdot}4$.**

## INTRODUCTION

Attractive intermolecular interactions between $\pi$-systems control the formation of different intermolecular complexes.[1,2] Aggregation of dyes,[3] stacking of aromatic molecules in crystals,[4] formation of host–guest complexes,[5] stabilization of double-helical DNA structures[6] and intercalation of $\pi$-systems into DNA[7] or graphite[8] have been attributed to intermolecular attractive $\pi$-interactions. Electron donor–acceptor interactions between $\pi$-systems provide an important driving force for the formation of intermolecular complexes. The oxidation and reduction potentials of the components control the stabilities of the resulting complexes,[9] although other interactions, such as electrostatic attraction or repulsion between the components, could contribute to the stabilization or destabilization, respectively, of the resulting complexes.[10]

Aggregation of porphyrins has been studied extensively both experimentally[11–13] and theoretically.[14,15] Porphyrin aggregates play an important role in the photosynthetic reaction centre, where two bacteriochlorophyll molecules interact strongly, and their fixed orientation assists charge separation.[16,17] Theoretical models suggest that the interactions between the bacteriochlorophyll units result from a combination of exciton coupling and charge-transfer transitions. Recent advances in organic synthesis have permitted the preparation of stable porphyrin analogues such as the tetrathiaporphyrin dication,[18] the tetraoxaporphyrin dication[19] and the tetraoxaporphycene dication,[20] which exhibit aromatic character. In a recent study we reported on the formation of intermolecular donor–acceptor complexes between the octaethyltetrathiaporphyrin dication (**1**), $OTP^{2+}$, and a series of $\pi$-donors.[21] It was shown that $OTP^{2+}$ forms 1:1 complexes with these $\pi$-donors and that the intermolecular interactions are primarily controlled by charge transfer.

In this paper, we report on the formation of intermolecular complexes between $OTP^{2+}$ and octaethylpor-

* Author for correspondence.

CCC 0894–3230/95/100659–12


*Received 28 December 1994*
*Revised 7 June 1995*

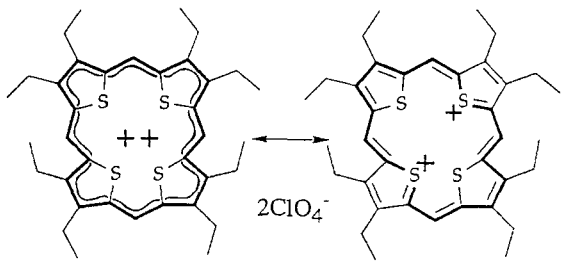


(1)

phyrin, (**2**), $H_2OEP$, and metal-substituted octaethylporphyrins $Ni^{II}$-OEP (**3**), $V^{IV}O$-OEP (**4**), and $Fe^{III}$-OEP chloride (**5**). Different types of intermolecular aggregates are formed between $OTP^{2+}$ and OEP. A primary, kinetically controlled, intermolecular aggregate, exhibiting the stoichiometry $(OTP^{2+})_2H_2OEP$, was detected. This complex rearranges to a thermodynamically stabilized aggregate of stoichiometry $(OTP^{2+})_4H_2OEP$. We characterized spectroscopically the kinetics associated with the different complexes and determined their association constants and the energy barrier for interconversion of the two complexes. We also found that the $OTP^{2+}$–$M^{n+}$-OEP complexes exhibit a 1:1 intermolecular stoichiometry and that charge-transfer and electrostatic interactions affect the stabilities of the intermolecular assemblies.

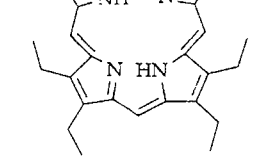


(2)

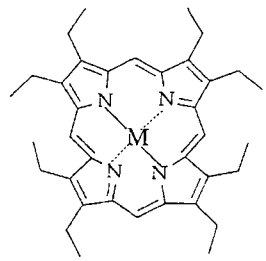


(3) M = Ni(II)
(4) M = V(IV)O
(5) M = Fe(III)

## EXPERIMENTAL

Absorption spectra were recorded on a Uvikon-860 spectrophotometer (Kontron) equipped with a thermostated cell holder. Cyclic voltammetric experiments were performed with a PAR Model 263 electroanalyzer (EG & G). The electrochemical cell consisted of a Pt working electrode (area 0·008 $cm^2$), a Pt wire as a counter electrode and a saturated calomel electrode (SCE) as a reference electrode. Electrochemical experiments were performed in dry $CH_2Cl_2$ and tetrabutylammonium tetrafluoroborate was used as the electrolyte. $^1H$ NMR spectra were recorded on a Bruker AMX-400 spectrometer at 400·135 MHz in $CD_2Cl_2$ solution at 297 K. *Chemical shifts are in ppm relative to* $\delta_{CHDCl_2} = 5{\cdot}281$. Octaethyltetrathiaporphyrin dication (perchlorate salt), $OTP^{2+}$, was prepared[22] by the acid-catalysed condensation of 3,4-diethyl-2-hydroxymethylthiophene, to yield octaethyltetrathiaporphyrinogen, and subsequent treatment of the latter with 2,3-dichloro-5,6-dicyano-*p*-benzoquinone and perchloric acid to yield $OTP^{2+}(ClO_4^-)_2$. All other chemicals were obtained from Aldrich.

Association constants of $OTP^{2+}$ with $[M^{n+}$-$OEP]^{(n-2)+}$ were determined spectroscopically in $CH_2Cl_2$ at 298 K. To a solution of $OTP^{2+}$ ($1{\cdot}8 \times 10^{-5}$ M) were added successively portions of an $M^{n+}$-OEP stock solution. Identical volumes of the $[M^{n+}$-$OEP]^{(n-2)+}$ stock solution were added to the $OTP^{2+}$ solution and to the reference cell that contained a similar volume of solvent present in the measuring cell. After each addition of $[M^{n+}$-$OEP]^{(n-2)+}$, the cell was allowed to equilibrate for 10 min at 298 K and the respective spectra were recorded. The recorded spectra were subtracted from the original $OTP^{2+}$ spectrum, and the association constants were calculated using the Benesi–Hildebrand relation (see text).

The kinetic analyses of the formation of the $OTP^{2+}$–$H_2OEP$ intermolecular complexes were carried out spectroscopically. The measuring cell included a solution of $OTP^{2+}$ ($1{\cdot}4 \times 10^{-5}$ M), and different concentrations of an $H_2OEP$ stock solution in $CH_2Cl_2$ were added to the measuring cell and the reference cell that contained a similar volume of the pure solvent to that of the measuring cell. The changes in absorption at $\lambda = 386$, 406 and 452 nm were recorded at time intervals for each concentration of $H_2OEP$. It should be noted that control experiments where the spectra of separated solutions of $H_2OEP$ and $OTP^{2+}$ were added and subtracted from the experimental spectrum formed on addition of $H_2OEP$ to $OTP^{2+}$ resulted in spectral changes in the $OTP^{2+}$ spectrum and the absorbance of $H_2OEP$ is unaffected ($\Delta OD < 0{\cdot}04$) (OD = optical density). This observation is valid at $H_2OEP$ concentrations $< 5 \times 10^{-6}$ M, and justifies the experimental method in which $H_2OEP$ is added to the reference cell to observe pure spectral changes in the

$OTP^{2+}$ absorbance. These control experiments indicate also that the spectral changes of $OTP^{2+}$ are not distorted as a result of spectral changes that could be associated with $H_2OEP$ as a result of complexation. The temperature in these experiments was kept constant at 298 K.

The procedures for the determination of the rate constants in the formation of the complexes, their association constants and the respective intermolecular stoichiometries are outlined in the text.

## RESULTS AND DISCUSSION

Octaethyltetrathiaporphyrin dication, $OTP^{2+}$ (**1**), exhibits two quasi-reversible one-electron reduction processes:

$$OTP^{2+} + e \rightleftharpoons OTP^{+\cdot} \quad (1)$$

$$OTP^{+\cdot} + e \rightleftharpoons OTP^{0} \quad (2)$$

The electron-acceptor properties of $OTP^{2+}$ suggest that it could stabilize donor–acceptor charge-transfer complexes. We studied the formation of intermolecular complexes (or aggregates) between $OTP^{2+}$ and electron-donating metal-octaethylporphyrins: $Ni^{II}$-OEP (**2**), $V^{IV}O$-OEP (**3**) and $Fe^{III}$-$OEP^+$ (**4**). The cyclic voltammograms of these metalloporphyrins are shown in Figure 1. These complexes reveal reversible $1e^-$ oxidation waves, implying their donating properties upon interaction with electron acceptors.

Figure 2 shows the spectral changes of $OTP^{2+}$ on addition of different concentrations of $Fe^{III}$-$OEP^+$ (**4**). In this experiment, **4** was added in equal concentrations to the $OTP^{2+}$ cell and the reference cell, so that the spectral changes arose only from $OTP^{2+}$. Control experiments in which the added spectra of separated solutions of $[M^{n+}\text{-OEP}]^{(n-2)+}$ (concentration $<6 \times 10^{-6}$ M) and $OTP^{2+}$ was subtracted from the experimental spectrum of the mixture of $[M^{n+}\text{-OEP}]^{(n-2)+}$ and $OTP^{2+}$ revealed that the $OTP^{2+}$ absorbance bands are affected whereas the absorbance band of $[M^{n+}\text{-OEP}]^{(n-2)+}$ is only slightly affected ($\Delta OD < 0{\cdot}05$). The absorption band of $OTP^{2+}$ ($\lambda = 452$ nm) decreases with the concomitant formation of new bands at $\lambda = 380$ nm and a charge-transfer band at $\lambda = 746$ nm. The appearance of isosbestic points in the $OTP^{2+}$ spectrum on addition of **4** indicates that $OTP^{2+}$ is transformed into a single intermolecular complex on addition of **4**.

The spectral changes observed on addition of **4** to $OTP^{2+}$ can be analysed in terms of the formation of a 1:1 intermolecular complex:

$$OTP^{2+} + D \overset{K_a}{\rightleftharpoons} (OTP^{2+} \cdots D] \quad (3)$$

where $D = [M^{n+}\text{-OEP}]^{(n-2)+}$. Provided that the intermolecular complex exhibits a 1:1 stoichiometry, the

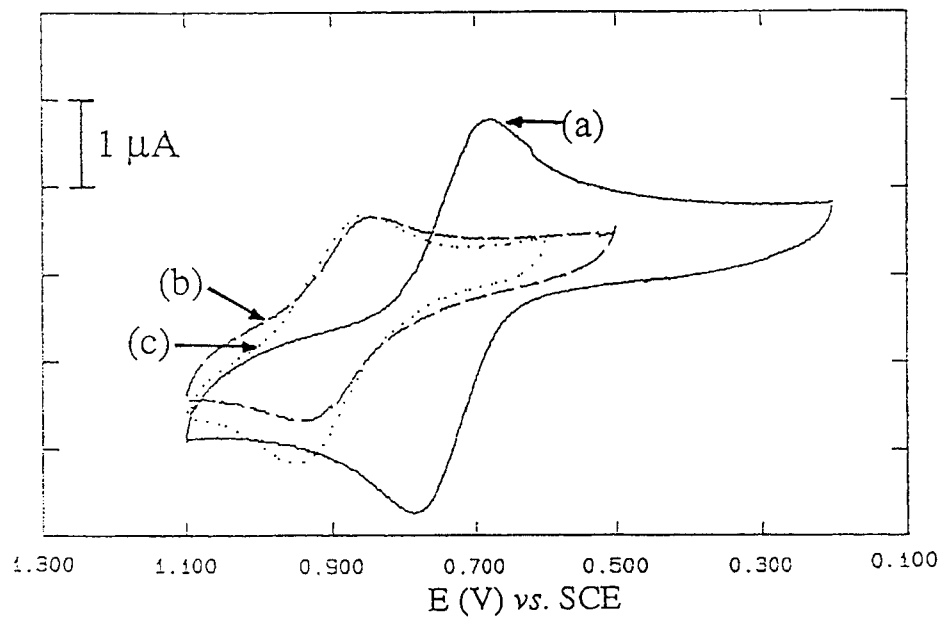


Figure 1. Cyclic voltammograms of (a) $Ni^{II}$-OEP, $5 \times 10^{-4}$ M, (b) $V^{IV}O$-OEP, $3 \times 10^{-4}$ M and (c) $Fe^{III}$-$OEP^+$, $3 \times 10^{-4}$ M, in $CH_2Cl_2$. Tetrabutylammonium tetrafluoroborate (0·01 M) was used as electrolyte. Scan rate = 100 mV $s^{-1}$

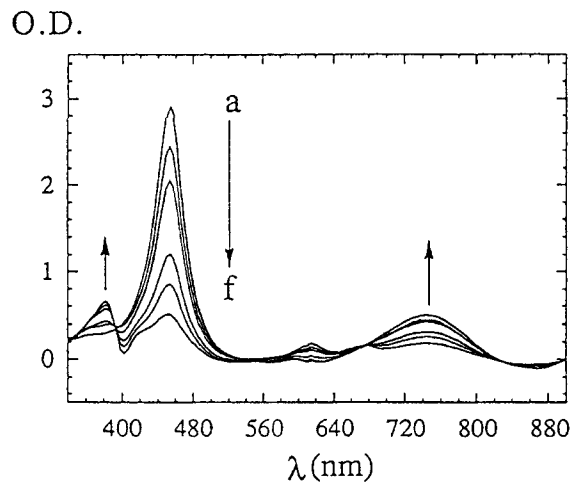


Figure 2. Absorption spectra of $OTP^{2+}$ ($1{\cdot}8\times10^{-5}$ M) in $CH_2Cl_2$ on addition of different amounts of $Fe^{III}$-$OEP^+$: (a) 0, (b) $2{\cdot}3\times10^{-6}$, (c) $4{\cdot}3\times10^{-6}$, (d) $8{\cdot}5\times10^{-6}$, (e) $1{\cdot}0\times10^{-5}$ and (f) $1{\cdot}3\times10^{-5}$ M. The concentration of $Fe^{III}$-$OEP^+$ was maintained at similar values in the measuring cell and reference cell

association constant of the complex will be given by

$$\frac{[OTP^{2+}]_0[D]_0}{\Delta OD} = \frac{1}{K_a\,\Delta\varepsilon} + \frac{1}{\Delta\varepsilon}([OTP^{2+}]_0 + [D]_0) \quad (4)$$

where ΔOD is the difference in absorbance between the complex and free $OTP^{2+}$, at any analytical concentration of $OTP^{2+}$, $[OTP^{2+}]_0$, and metal porphyrin electron donor, $[D]_0$, respectively. $\Delta\varepsilon$ is the difference between the molar extinction coefficient of the complex and the sum of the molar extinction coefficients of the free electron acceptor ($OTP^{2+}$) and free electron donor $[M^{n+}\text{-}OEP]^{(n-2)+}$ at the wavelength of the absorbance measurement.[23]

Figure 3 shows the graphical analysis of the spectral changes shown in Figure 2 in terms of equation (4). A linear relationship between $[OTP^{2+}]_0[D]_0/\Delta OD$ and $[OTP^{2+}]_0 + [D]_0$ is obtained, implying the formation of a 1:1 intermolecular complex. From the slope and intercept, the association constant of the complex was derived and its value is $K_a = 6{\cdot}7\times10^4$ $M^{-1}$. The other metal porphyrins (**2** and **3**) revealed similar spectral changes that were consistent with formation of a 1:1 intermolecular complex stoichiometry. Table 1 summarizes the derived values of the association constants of the different complexes and the difference in the half-wave potentials of the donor and acceptor components of the complexes. It should be noted that metal-OEP complexes that do not act as electron donors, e.g. $Fe^{II}$-OEP, or poor electron-donor metal porphyrins, e.g.

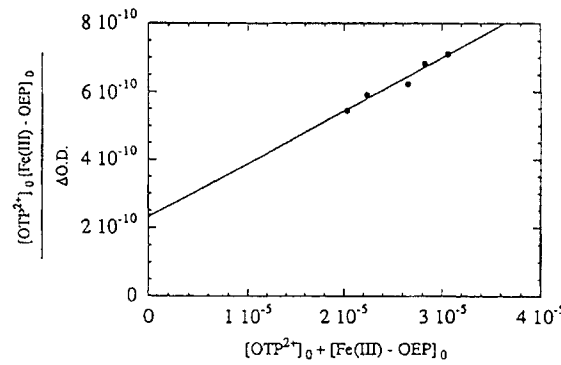


Figure 3. Benesi–Hildebrand plot for the association of $Fe^{III}$-$OEP^+$ to $OTP^{2+}$, according to equation (4) and using data in Figure 2 at $\lambda = 742$ nm

$Fe^{III}$-*meso*-tetraphenylporphyrin chloride, did not form intermolecular complexes with $OTP^{2+}$ (**1**).

The association constants of donor–acceptor complexes are governed by various parameters such as solvent polarity and electron-donating and -accepting affinities of the components of the complex. The difference in the half-wave potentials ($\Delta E_{1/2}$) of the electron donor and electron acceptor comprising the complex reflects the thermodynamic driving force for the formation of the intermolecular assembly. Accordingly, we realize that the association constant of $V^{IV}O$-OEP (**4**) to $OTP^{2+}$ is approximately twice that of $Ni^{II}$-OEP (**2**) ($\Delta E_{1/2} = 0{\cdot}52$ vs 0·32 V). Nonetheless, although the driving force for the formation of $V^{IV}O$-OEP and $Fe^{III}$-$OEP^+$ complexes is very similar, the association constant of the latter metal porphyrin is approximately half that of **4**. This is attributed to electrostatic repulsions between $OTP^{2+}$ and $Fe^{III}$-$OEP^+$ that perturb the stabilization of the intermolecular complex.

The formation of the intermolecular assembly between $OTP^{2+}$ and the metal-free ligand octaethylporphyrin $H_2OEP$ (**2**) reveals interesting features that are not detected with the metal-OEP. Figure 4 shows (a) the absorption spectrum of $OTP^{2+}$ and (b) the absorption

Table 1. Association constant of $OTP^{2+}$–π-donors[a] and donor–acceptor half-wave potential differences[b]

| Substrate | $K_a$ ($M^{-1}$) | $\Delta E_{1/2}$ (V) |
|---|---|---|
| $Ni^{III}$-OEP | 700 000 | 0·36 |
| $V^{IV}O$-OEP | 142 000 | 0·52 |
| $Fe^{III}$-$OEP^+$ | 67 000 | 0·53 |

[a] Values measured in $CH_2Cl_2$.
[b] $\Delta E_{1/2} = E_{1/2}$ (π-donor) – $E_{1/2}$ (electron acceptor). $E_{1/2}$ of electron acceptor, $OTP^{2+}$, corresponds to 0·37 V vs SCE in $CH_2Cl_2$.

spectral changes of $OTP^{2+}$, as a function of time, on addition of $H_2OEP$ ($2{\cdot}0 \times 10^{-6}$ M). On addition of $H_2OEP$ the maximum absorption band of $OTP^{2+}$ ($\lambda_{max} = 452$ nm) decreases in its intensity with the simultaneous formation of a charge-transfer (CT) band at $\lambda = 742$ nm. A new absorption band corresponding to the formation of an intermolecular complex is observed at $\lambda_{max} = 386$ nm. This absorption band increases in its intensity as a function of time. The band at $\lambda_{max} = 386$ nm reaches a maximum value and undergoes further changes. After a longer time the band at $\lambda_{max} = 386$ nm decreases in its intensity and a new band is formed at $\lambda_{max} = 406$ nm [Figure 4(c)]. This latter band increases with time with the simultaneous enhancement of the CT band at $\lambda = 742$ nm. The absorption band at $\lambda = 386$ nm almost disappears, although a residual band is detected after the system has reached equilibrium. The disappearance of the band at $\lambda_{max} = 386$ nm and formation of the band at $\lambda_{max} = 406$ nm are accompanied by a further decrease in the absorbance band of the parent $OTP^{2+}$, $\lambda_{max} = 452$ nm. Figure 5 shows the absorbance changes of the three different bands as a function of time. Evidently, after long time intervals a steady-state equilibrium between free $OTP^{2+}$ ($\lambda_{max} = 452$ nm) and an intermolecular assembly with $H_2OEP$ ($\lambda_{max} = 406$ nm) is formed. These results suggest that on addition of $H_2OEP$ to $OTP^{2+}$ an intermolecular, kinetically controlled complex is formed ($\lambda_{max} = 386$ nm, species X) which is transformed into a thermodynamically stabilized intermolecular assembly ($\lambda_{max} = 406$ nm, species Y).

A further qualitative insight into the nature of these two intermolecular complexes is obtained on examination of the effect of added $H_2OEP$ on the thermodynamically stabilized complex. Figure 6 shows the absorption spectrum of the thermodynamically stabilized complex ($\lambda_{max} = 406$ nm) formed on the first addition of $H_2OEP$, as described above, and the spectral changes of the system as a function of time, on addition of a further quantity of $H_2OEP$. Immediately on addition of $H_2OEP$, the absorption band at $\lambda_{max} = 406$ nm decreases in intensity and the absorption band at $\lambda_{max} = 386$ nm increases. Following this rapid spectral change, the band at $\lambda_{max} = 386$ nm decreases in intensity and the band at $\lambda = 406$ nm increases as time proceeds.

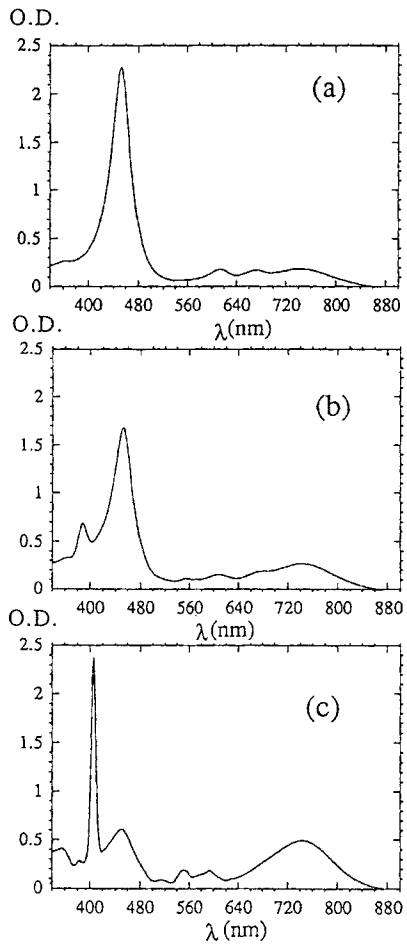


Figure 4. Absorption spectra of (a) $OTP^{2+}$ ($1{\cdot}4 \times 10^{-5}$ M) in $CH_2Cl_2$, (b) $OTP^{2+}$ ($1{\cdot}4 \times 10^{-5}$ M) recorded 6 min after addition of $H_2OEP$ ($2 \times 10^{-6}$ M) and (c) $OTP^{2+}$ ($1{\cdot}4 \times 10^{-5}$ M) recorded 40 min after the addition of $H_2OEP$ ($2 \times 10^{-6}$ M). In experiments (b) and (c) $H_2OEP$ ($2 \times 10^{-6}$ M) was also added to the reference cell, and the recorded spectra represent the net changes in $OTP^{2+}$ absorbance bands

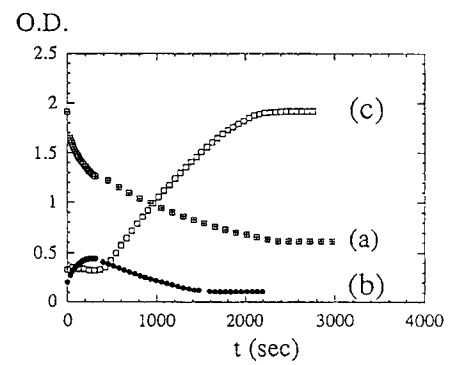


Figure 5. Absorbance changes of $OTP^{2+}$ and its intermolecular complexes as a function of time. (a) Absorbance at $\lambda = 452$ nm, reflecting the concentration of $OTP^{2+}$; (b) absorbance at $\lambda = 386$ nm, reflecting the concentration of $A_2D$; (c) absorbance at $\lambda = 406$ nm, reflecting the concentration of $A_4D$

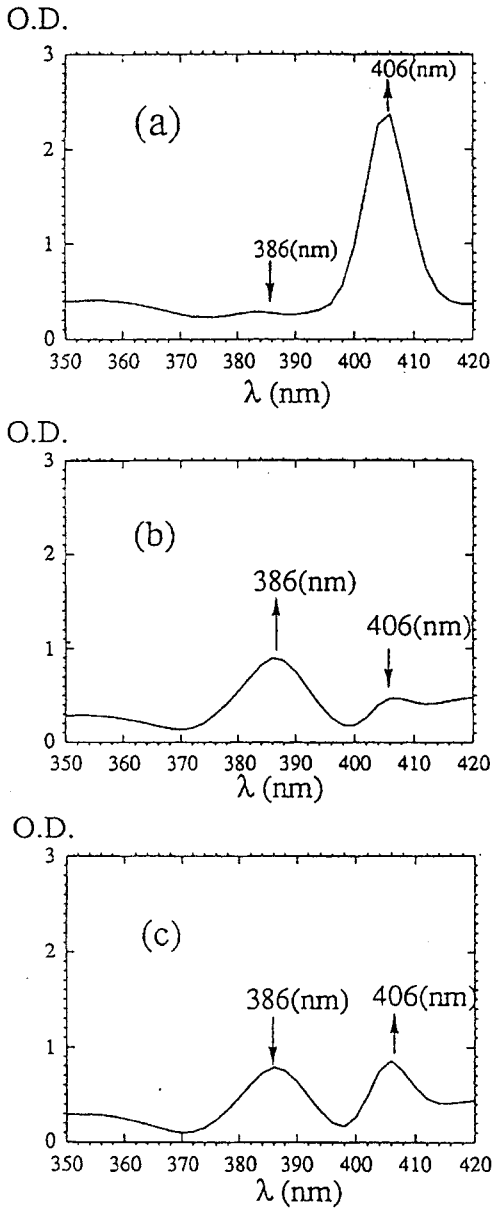


Figure 6. (a) Absorption spectrum of $OTP^{2+}$ ($1{\cdot}4 \times 10^{-5}$ M) and $H_2OEP$ ($2 \times 10^{-6}$ M) after 40 min. (b) Absorption spectrum resulting on addition of $H_2OEP$, ($2 \times 10^{-6}$ M) to the system in (a). The spectrum was recorded immediately after addition of $H_2OEP$. (c) Absorption spectrum of the system in (b) after 40 min of equilibration. In all experiments $H_2OEP$ concentration was maintained at similar values in the analysing and reference cells. Hence the absorption spectra reflect to the absorbance change of $OTP^{2+}$ only. All measurements were conducted in $CH_2Cl_2$

The new steady-state equilibrium formed after the second addition of $H_2OEP$ reveals, however, that the two intermolecular assemblies between $OTP^{2+}$ and $H_2OEP$ exist in equilibrium. At the higher $H_2OEP$ concentration the [species Y]/[species X] equilibrium ratio is lower than at the lower $H_2OEP$ concentration. These descriptive results already provide some insight into the nature of the different intermolecular complexes formed between $OTP^{2+}$ and $H_2OEP$. The results indicate that species X ($\lambda_{max} = 386$ nm) and species Y ($\lambda = 406$ nm) yield a steady-state equilibrium. Further, the results imply that the transformation of species X to species Y involves the dissociation of one or more $H_2OEP$ unit from the primary intermolecular assembly. This conclusion is based on the fact that species X is formed from species Y on addition of $H_2OEP$, and on the observed steady-state enrichment of species X at higher $H_2OEP$ concentrations. It should be noted that attempts to analyse the absorbance changes of $OTP^{2+}$ on addition of $H_2OEP$ in terms of a 1:1 complex failed to give the expected linear relationship expressed in equation (4).

For quantitative analysis of the stoichiometries involved in the different complexes, for the determination of the rate constant for transformation of species X to species Y, and for the extraction of the association constants of the different intermolecular assemblies and the equilibrium constant between species X and species Y, we assume that the primary complex (species X) involves two acceptor units ($OTP^{2+}$) and one donor unit ($H_2OEP$):

$$2A + D \underset{k_{-1}}{\overset{k_1}{\rightleftharpoons}} A_2D$$

$$K_1 = \frac{k_1}{k_{-1}} = \frac{[A_2D]}{[A]^2[D]} \qquad (5)$$

where A represents $OTP^{2+}$ and D represents $H_2OEP$. Calculation of the kinetic and thermodynamic parameters associated with the primary complex is based on the fact that the absorbance bands of the parent $OTP^{2+}$ and the bands of the primary and secondary complexes do not overlap. Furthermore, Figure 5 shows that the absorbance changes of the absorption bands of $OTP^{2+}$ and of the two complexes at time intervals after addition of $H_2OEP$ reveal an important feature that facilitates the analysis. We see that after a short time (up to *ca* 360 s) only the primary complex is formed and the concentration of the secondary complex is essentially zero. Thus, at short time intervals the decrease in the absorbance of $OTP^{2+}$ ($\lambda = 452$ nm) and build-up of the band at $\lambda = 386$ nm reflect the kinetics of the formation of the primary complex only. Assuming the stoichiometry given in equation (5) for the primary complex, the rate expression for the formation of the primary complex is

given by

$$\frac{1}{[A]_0 - 2[D]_0} \ln \frac{[A]_0 - 2[A_2D]}{[D]_0 - [A_2D]} - \frac{1}{[A]_0 - 2[A_2D]} = k_1([A]_0 - 2[D]_0)t + C \quad (6)$$

where $[A]_0$ and $[D]_0$ are the analytical concentrations of $OTP^{2+}$ and $H_2OEP$ respectively, in the system, $[A_2D]$ is the intermolecular complex concentration at any time interval and $C$ is a constant (see Appendix). As the molar extinction coefficient of $OTP^{2+}$ is known ($\lambda_{max} = 452$ nm, $\varepsilon = 1{\cdot}59 \times 10^5\ M^{-1}cm^{-1}$), the concentration of the complex, $[A_2D]$, after a short time can be expressed by the decrease in the absorption band of $OTP^{2+}$, according to

$$[A_2D] = -\Delta OD_{452}/2\varepsilon^{A}_{452} \quad (7)$$

(see appendix). Figure 7 shows the changes in $[A_2D]$ according to equation (6). A linear relationship is obtained as expected for an $A_2D$ stoichiometry. The derived rate constant is $k_1 = 1{\cdot}9 \times 10^7\ s^{-1}M^{-2}$. It should be noted that attempts to analyse the decay of $OTP^{2+}$ using expressions corresponding to other stoichiometries failed to give appropriate linear correlations. Thus, the stoichiometry of the primary complex, $A_2D$, is supported by the kinetic analysis of its formation.

The association constant, $K_1$, of the primary complex $A_2D$ can be determined from the first steady-state equilibrium that corresponds to $A_2D$. Figure 5 shows the absorption changes of $OTP^{2+}$ and $A_2D$ at time intervals after addition of $H_2OEP$, $4{\cdot}66 \times 10^{-6}$ M, to an $OTP^{2+}$ solution. We see that after 360 s the absorbance of the complex $A_2D$ reaches a maximum value and the secondary complex is not yet formed. Hence this peak absorbance corresponds to the steady-state equilibrium of $A_2D$. The decrease in the $OTP^{2+}$ band (452 nm) at the time interval of the maximum absorbance of $A_2D$

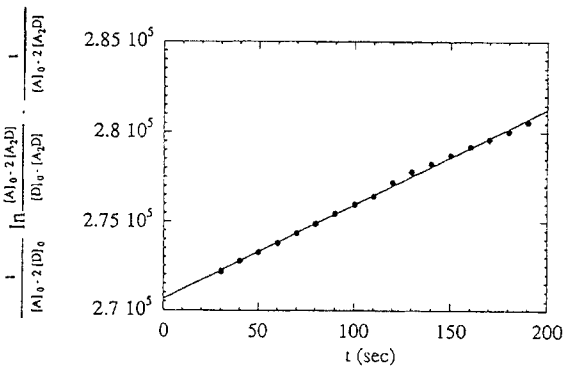


Figure 7. Kinetic analysis for the formation of the intermolecular complex $A_2D$ according to equation (6). The concentration of $[A_2D]$ was determined from data in Figure 5

allows the determination of $[A_2D]$, [D] and [A] at equilibrium ($[OTP^{2+}]_0$ and $[H_2OEP]_0$ are known and $\varepsilon_{452} = 1{\cdot}59 \times 10^5\ M^{-1}cm^{-1}$). The derived association constant of the complex $A_2D$ corresponds to $K_1 = 1{\cdot}3 \times 10^{10}\ M^{-2}$.

The secondary intermolecular $OTP^{2+}$–$H_2OEP$ complex (species Y) originates, as stated earlier, by dissociation of the donor component. Among several possible dissociation pathways, we assume that one donor unit dissociates on aggregation of two intermolecular complexes of structure $A_2D$, according to equation (8), and the association constant of the secondary complex is then expressed in terms of equation (9).

$$2A_2D \underset{k_{-2}}{\overset{k_2}{\rightleftharpoons}} A_4D + D \quad (8)$$

$$K_2 = \frac{[A_4D][D]}{[A_2D]^2} \quad (9)$$

To support the suggested stoichiometry of the secondary intermolecular complex (species Y), we analyse the rate of its formation from species X ($A_2D$) at times far from equilibrium. The rate of formation of the secondary complex $A_4D$ is given by

$$\frac{d[A_4D]}{dt} = k_2[A_2D]^2 \quad (10)$$

The differences in absorbance between the spectrum of pure $OTP^{2+}$ and the resulting spectrum on addition of $H_2OEP$, at any wavelength and at any time of formation of the two complexes, $\Delta OD_\lambda$, is given by

$$\Delta OD_\lambda = a_\lambda[A_2D] + b_\lambda[A_4D] \quad (11)$$

where $a_\lambda$ and $b_\lambda$ are expressed by

$$a_\lambda = \varepsilon_\lambda^{A_2D} - \varepsilon_\lambda^{D} - 2\varepsilon_\lambda^{A} \quad (12)$$

$$b_\lambda = \varepsilon_\lambda^{A_4D} - 4\varepsilon_\lambda^{A} - \varepsilon_\lambda^{D} \quad (13)$$

where $\varepsilon_\lambda^{A}$, $\varepsilon_\lambda^{D}$, $\varepsilon_\lambda^{A_2D}$ and $\varepsilon_\lambda^{A_4D}$ represent the molar extinction coefficients of A, D, $A_2D$ and $A_4D$, respectively, at any absorbance wavelength. [This relationship is correct under the specific experimental conditions where $H_2OEP$ is added at a similar concentration to the analysing cell and reference cell. Under these conditions, the absorbance differences are only detectable in the spectrum of $OTP^{2+}$ (see Experimental section).] Thus, equation (11) allows us to express the concentration of $A_2D$ in terms of the secondary complex concentration $A_4D$:

$$[A_4D] = \frac{\Delta OD_\lambda - b_\lambda[A_4D]}{a_\lambda} \quad (14)$$

This relationship could then be substituted in equation (10) and enables us to derive a rate equation for $A_4D$.

Figure 5 shows the absorbance changes ($\Delta OD_\lambda$) of the system at various times of formation of the different complexes $A_2D$ and $A_4D$. Fortunately, we detect a time window where the complex $A_4D$ is formed, as is evident from the increase in absorbance at 406 nm, but the absorbance difference at $\lambda = 386$ nm exhibits a constant value between 2300 and 15000 s. This allows us to integrate equation (10) and to express the concentration of $A_4D$ in terms of the absorbance difference at $\lambda = 386$ nm, $\Delta OD_{386}$, $a_{386}$ and $b_{386}$, according to

$$\frac{1}{\Delta OD_{386} - b_{386}[A_4D]} = \frac{b_{386}}{(a_{386})^2} k_2 t + \text{constant} \quad (15)$$

Thus, in order to derive the rate constant for the formation of the secondary complex, the concentration of $A_4D$ as a function of time and the values of $a_{386}$ and $b_{386}$ must be determined. The value of $a_{386}$ is easily determined by plotting $\Delta OD_{386}$ vs $[A_2D]$ at time intervals where $A_4D$ is not yet formed [cf. equation (11)]. The slope corresponds to $a_{386}$ and exhibits the value $a_{386} = 1{\cdot}78 \times 10^5\ M^{-1}\,cm^{-1}$. The concentration of $[A_4D]$ at any time interval can be evaluated by solving the two equations representing the absorbance changes at $\lambda = 452$ and 386 nm:

$$\Delta OD_{452} = -2\varepsilon^{A}_{452}[A_2D] - 4\varepsilon^{A}_{452}[A_4D] \quad (16)$$

$$\Delta OD_{386} = a_{386}\,[A_2D] + b_{386}[A_4D]$$
$$= 1{\cdot}78 \times 10^5[A_2D] + (-\varepsilon^{D}_{386} - 2\varepsilon^{A}_{386})[A_4D] \quad (17)$$

In formulation of equation (17), we refer to the fact that $\varepsilon^{A_4D}_{386} \approx 0$ since the complex $A_4D$ does not exhibit any absorbance at $\lambda = 386$ nm, and hence $b_{386} = -\varepsilon^{D}_{386} - 2\varepsilon^{A}_{386}$. By solving this set of equations for any time, one can derive the respective concentration of the secondary complex, $[A_4D]$. Furthermore, the general equation of the absorbance difference at any wavelength, equation (11), implies that the value of $a$ at $\lambda = 406$ nm is zero, $a_{406} = 0$. This conclusion is based on the experimental result that indicates that $\Delta OD_{406} = 0$ after short times when only the complex $A_2D$ is formed. Thus, the concentration of $A_4D$ is expressed by the absorbance difference at $\lambda = 406$ nm:

$$\Delta OD_{406} = b_{406}[A_4D] \quad (18)$$

Hence the concentration of $A_4D$ deduced by solving equations (16) and (17) allows us to calculate $b_{406}$ and its value is $9{\cdot}34 \times 10^5\ M^{-1}\,cm^{-1}$. Knowing the value of $b_{406}$ and using equation (18), the determination of $A_4D$ at any time interval is trivial. Figure 8 shows the plot of $1/(\Delta OD_{396} - b_{386}[A_4D])$ vs time. A linear relationship is obtained as predicted for the kinetic analysis corresponding to the formation of an intermolecular complex exhibiting the stoichiometry $A_4D$, equation (15). From the slope and the values of $b_{386}$ and $a_{386}$, the rate constant for the formation of $A_4D$ is $k_2 = 1500\ M^{-1}\,s^{-1}$.

The association constant of the secondary intermolecular complex, $K_2$, equation (9), was determined by calculating the concentrations of $A_4D$ and $A_2D$ at equilibrium. From the respective $\Delta OD$ values and using equations (17) and (18), the values of $[A_2D]$, $[A_4D]$ and $[D]$ at equilibrium were calculated ($[D] = [D]_0 - [A_2D] - [A_4D]$). Substitution of these values into equation (9) gives $K_2 = 7{\cdot}4$ as the equilibrium constant between the secondary and primary intermolecular complexes.

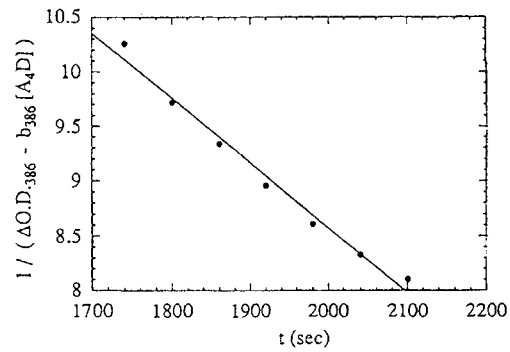


Figure 8. Kinetic analysis for the formation of the complex $A_4D$ according to equation (15). The concentration of $[A_4D]$ was calculated from data in Figure 5 using equation (18)

The analysis for the determination of $k_2$ and $K_2$ was carried out by following the absorbance differences of $OTP^{2+}$ ($1{\cdot}2 \times 10^{-5}$ M) on addition of $H_2OEP$ ($4{\cdot}66 \times 10^{-6}$ M) (Figure 5). On increasing the amount of $H_2OEP$ added to the initial $OTP^{2+}$ solution, similar time-dependent absorbance-difference profiles are observed, although the time required for the initiation of the formation of $A_4D$ and the ultimate equilibrium $\Delta OD$ values change. Analysis of these plots according to the method described here for one $H_2OEP$ concentration yielded identical $k_2$ and $K_2$ values. Furthermore, attempts to analyse the absorbance changes at $\lambda = 406$ nm in terms of other stoichiometries and the respective rate expressions failed to give appropriate linear relationships. We therefore conclude that the kinetic analysis of the absorbance changes associated with the formation of the secondary complex strongly support the formation of an intermolecular donor–acceptor assembly of $A_4D$ stoichiometry.

The activation barrier associated with the formation of the secondary complex was also investigated. Whereas the primary rate constant ($k_1$) corresponding to the primary complex $A_2D$ is not affected within the temperature range 278–298 K, the rate constant for the formation of the secondary complex, $A_4D$, is temperature dependent. From the Arrhenius plot corresponding to the rate of formation of the intermolecular assembly $A_4D$, the activation energy ($E_a$) associated with the transformation of the primary complex $A_2D$ to $A_4D$ is 16·5 kcal mol$^{-1}$ (1 kcal = 4·184 kJ).

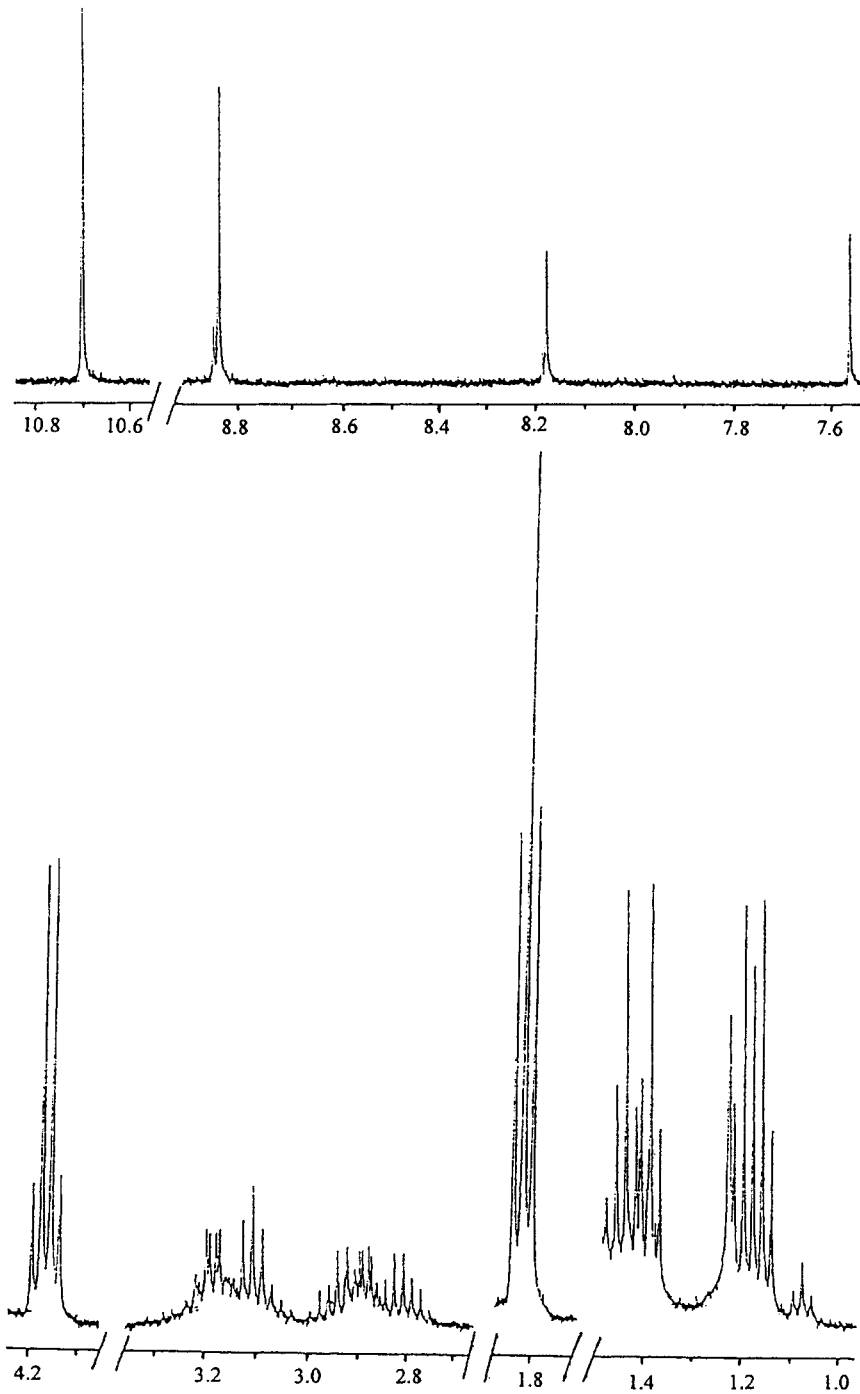


Figure 9. $^1H$ NMR spectrum of a mixture of $OTP^{2+}$ ($2{\cdot}26 \times 10^{-3}$ M) and $H_2OEP$ ($3{\cdot}9 \times 10^{-4}$ M). The spectrum of free $OTP^{2+}$ in the system has been deleted for simplification

Table 2. $^1$H NMR assignments for $OTP^{2+}$, $H_2OEP$ and $OTP^{2+}$–$H_2OEP$ intermolecular complexes[a]

| | | | $A_2D$ | | $A_4D$ | |
|---|---|---|---|---|---|---|
| | $OTP^{2+}$ | $H_2OEP$ | $OTP^{2+}$ | $H_2OEP$ | $OTP^{2+}$ | $H_2OEP$ |
| Aromatic | 12·187 (s) | 10·107 (s) | 8·82 (s) | 8·17 (s) | 10·7 (s) | 7·57 (s) |
| $CH_2$ | 4·453 (q) | 4·094 (q) | 3·2 (m) | 3·1 (m) | 4·16 (q) | 2·9 (m) |
| $CH_3$ | 1·964 (t) | 1·894 (t) | 1·4 (m) | 1·4 (m) | 1·82 (t) | 1·2 (m) |
| NH | – | −3·74 (s) | – | −4·73 (s) | – | −4·73 (s) |

[a] Chemical shifts in ppm relative to $\delta_{CHDCl_2} = 5{\cdot}281$.

Preliminary $^1$H NMR studies are compatible with the formation of $A_2D$ and $A_4D$ intermolecular complexes between $OTP^{2+}$ and $H_2OEP$. Figure 9 shows the $^1$H NMR spectrum obtained on equilibration of $OTP^{2+}$ ($2{\cdot}26 \times 10^{-3}$ M) and $H_2OEP$ ($1{\cdot}7 \times 10^{-4}$ M). Under these conditions, where $OTP^{2+}$ is used in excess, only the NMR signals corresponding to free $OTP^{2+}$ (not shown) and the intermolecular complex are detected. The 2D-NOESY spectrum yields NOE correlations between the aromatic singlets (7·5–10·8 ppm) and the $CH_2$ region (2·7–4·2 ppm) and COSY-type correlations between the $CH_2$ and $CH_3$ (1·1–1·9 ppm) regions. From the integrated areas of the $^1$H NMR signals and the 2D-NOESY correlations, we deduce the presence of two kinds of intermolecular complexes of stoichiometries corresponding to $A_2D$ and $A_4D$ in equilibrium. Table 2 summarizes the assignment of the $^1$H NMR spectrum for each of the complexes. It should be noted that in the aromatic region, two small singlets appear at 8·18 and 8·84 ppm next to the singlets corresponding to the aromatic protons of the complex $A_2D$. These signals presumably originate from an isomer of the intermolecular complex with the stoichiometry $A_2D$ that does not exchange rapidly with the major $A_2D$ species. Further studies to elucidate the structural relationships of the $A_2D$ and $A_4D$ complexes are, however, required.

## CONCLUSIONS

We have discussed the formation of intermolecular donor–acceptor complexes between the octaethylthiaporphyrin dication, $OTP^{2+}$, and metal complexes of octaethylporphyrin or the free ligand octaethylporphyrin, $H_2OEP$. With metal-substituted OEP, intermolecular donor–acceptor complexes of 1:1 stoichiometry are formed. The association constants of these complexes are controlled by the electron-donating properties of the metal-substituted OEP, and further influenced by electrostatic interactions prevailing in the molecular aggregates. The most interesting observations were detected on analysis of the intermolecular complexes formed between $OTP^{2+}$ and $H_2OEP$. The formation of a primary complex exhibiting the stoichiometry $(OTP^{2+})_2(H_2OEP)$ was observed, $\lambda_{max} = 386$ nm ($\varepsilon = 2{\cdot}94 \times 10^5$ M$^{-1}$ cm$^{-1}$). This complex transforms into a thermodynamically stabilized complex that involves a stoichiometry $(OTP^{2+})_4(H_2OEP)$, $\lambda_{max} = 406$ nm ($\varepsilon = 10{\cdot}24 \times 10^5$ M$^{-1}$ cm$^{-1}$). The activation energy associated with the formation of the latter complex is $E_a = 16{\cdot}5$ kcal mol$^{-1}$. Characterization of the detailed structures of these intermolecular complexes is under way.

## REFERENCES


1. F. Diederich, *Angew. Chem., Int. Ed. Engl.* **27**, 362 (1988).
2. (a) P. Calurie, in *Intermolecular Interactions: from Diatomics to Biopolymers*, edited by B. Pullman, p. 69. Wiley, Chichester (1978). (b) C. J. Bender, *Chem. Soc. Rev.* **15**, 475 (1986).
3. D. Valdes-Aquilera and D. C. Neckers, *Acc. Chem. Res.* **22**, 171 (1989).
4. G. R. Desiraju (Ed.), *Organic Solid-State Chemistry*. Elsevier, Amsterdam (1987).
5. (a) I. Willner, Y. Eichen, M. Rabinovitz, R. Hoffman and S. Cohen, *J. Am. Chem. Soc.* **114**, 637 (1992); (b) B. Askew, P. Ballester, C. Buhr, K. S. Jeong, S. Jones, K. Parris, K. Williams and J. Rebek, Jr, *J. Am. Chem. Soc.* **111**, 1082 (1989); (c) P. L. Anelli, P. R. Ashton, R. Balardini, V. Balzani, M. Delgado, M. T. Gandolfi, T. T. Goodnow, A. E. Kaifer, D. Philp, M. Pietraszkiewicz, L. Prodi, M. V. Reddington, A. M. Z. Slawin, N. Spencer, J. F. Stoddart, C. Vicert and D. J. Williams, *J. Am. Chem. Soc.* **114**, 193 (1992); (d) H.-J. Schneider, T. Blatter, S. Simova and I. Thesis, *J. Chem. Soc., Chem. Commun.* 580 (1989); (e) J. Jazwinski, A. J. Blacker, J.-M. Lehn, M. Cesario, J. Guilhem and C. Pascard, *Tetrahedron Lett.* **28**, 6057 (1987); (f) S. B. Ferguson and F.Diederich, *Angew. Chem., Int. Ed. Engl.* **25**, 1127 (1986).
6. A. H.-J. Wang, G. Ghetto, G. J. Quigley and A. Rich, *Biochemistry* **26**, 1152 (1987).
7. (a) H.-Y. Mei and J. K. Barton, *J. Am. Chem. Soc.* **108**, 7414 (1986); (b) C. V. Kumar, J. K. Barton and N. J. Turro, *J. Am. Chem. Soc.* **107**, 5518 (1985); (c) J. K. Barton, J. M. Goldberg, C. V. Kumar and N. J. Turro, *J.*

*Am. Chem. Soc.* **108**, 2081 (1986); (d) M. D. Purugganan, C. V. Kumar, N. J. Turro and J. K. Barton, *Science* **241**, 1645 (1988).
8. G. Lipiner, I. Willner and Z. Aizenshtat, *J. Chem. Soc., Chem. Commun.* 34 (1987).
9. (a) C. A. Hunter and J. K. M. Sanders, *J. Am. Chem. Soc.* **112**, 5525 (1990); (b) L. Foster, *Organic Charge-Transfer Complexes*. Academic Press, New York (1969); (c) M. W. Hanna and J. L. Lippert, in *Molecular Complexes*, edited by R. Foster, Vol. 1. Eleck Science, London (1973).
10. I. Willner, Y. Eichen, A. Doron and S. Marx, *Isr. J. Chem.* **32**, 53 (1992).
11. (a) W. I. White, in *The Porphyrins*, edited by D. Dolphin, Vol. 5, Part C, Chapt. 7. Academic Press, New York (1978); (b) D. L. Akins, H.-R. Zhu and C. Guo, *J. Phys. Chem.* **98**, 3612 (1994); (c) O. Ohno, Y. Kaizu and H. Kobayashi, *J. Chem. Phys.* **99**, 4128 (1983); (d) M. Krishnamurthy, J. R. Sutterr and P. Hambright, *J. Chem. Soc., Chem. Commun.* 13 (1975); (e) T. K. Chandrashekar, H. van Willigen and M. H. Ebersole, *J. Phys. Chem.* **88**, 4326 (1984); (f) E. B. Fleischer, J. M. Palmer, T. S. Srivastava and A. Chatterjee, *J. Am. Chem. Soc.* **93**, 3162 (1971).
12. (a) J. M. Ribo, J. Crusats, J.-A. Farrera and M. L. Valero, *J. Chem. Soc., Chem. Commun.* 681 (1994); (b) A. Corsini and O. Herrmann, *Talanta* **33**, 335 (1986); (c) M. Ravikant, D. Reddy and T. K. Chandrashekar, *J. Chem. Soc., Dalton Trans.* 2103 (1991).
13. (a) K. M. Smith (Ed.), *Porphyrins and Metalloporphyrins*. Elsevier, Amsterdam (1975); (b) R. F. Pasternack, *Ann. N.Y. Acad. Sci.* **206**, 614 (1973); (c) R. J. Abraham, F. Eivazi, H. Pearson and K. M. Smith, *J. Chem. Soc., Chem. Commun.* 698 (1976); 699 (1976); (d) J. W. Buchler, P. Hammerschmitt, I. Kaufeld and J. Loffler, *Chem. Ber.* **124**, 2151 (1991); (e) J. K. Duchowski and D. F. Bocian, *J. Am. Chem. Soc.* **112**, 8807 (1990); (f) J. W. Buchler, K. Elsässer, M. Kihn-Botulinski, B. Scharbert and S. Tancil, *ACS Symp. Ser.* **321**, 94 (1986); (g) J. W. Buchler, A. De Cian, J. Fischer, M. Kihn-Botulinski, H. Paulus and R. Weiss, *J. Am. Chem. Soc.* **108**, 3652 (1986); (h) J. W. Buchler and B. Scharbert, *J. Am. Chem. Soc.* **110**, 4272 (1988).
14. (a) C. A. Hunter, J. K. M. Sanders and A. J. Stone, *Chem. Phys.* **133**, 395 (1989); (b) J.-H. Perng, J. K. Duchowski and D. F. Bocian, *J. Phys. Chem.* **94**, 6684 (1990).
15. A. Warshel and W. W. Parson, *J. Am. Chem. Soc.* **109**, 6143 (1987); (b) W. J. Pietro, T. J. Marks and M. A. Ratner, *J. Am. Chem. Soc.* **107**, 5387 (1985).
16. (a) J. Deisenhofer, O. Epp, K. Miki, R. Huber and H. Michel, *J. Mol. Biol.* **108**, 385 (1984); (b) H. Michel, O. Epp and J. Deisenhofer, *EMBO J.* **5**, 2445 (1986).
17. J. P. Allen, G. Feher, T. O. Yeates, H. Komiya and D. C. Rees, *Proc. Natl. Acad. Sci. USA* **84**, 5730 (1986).
18. E. Vogel, P. Röhrig, M. Sicken, B. Knipp, A. Herrmann, M. Pohl, H. Schmickler and J. Lex, *Angew. Chem., Int. Ed. Engl.* **28**, 1651 (1989).
19. (a) E. Vogel, W. Hass and B. Knipp, *Angew. Chem., Int. Ed. Engl.* **27**, 406 (1988); (b) R. Bachmann, F. Gerson, G. Gescheidt and E. Vogel, *J. Am. Chem. Soc.* **114**, 10855 (1992).
20. (a) E. Vogel, M. Sicken, P. Röhrig, H. Schmrickler, J. Lex and O. Ermer, *Angew. Chem., Int. Ed. Engl.* **27**, 411 (1988); (b) R. Bachmann, F. Gerson, G. Gescheidt and E. Vogel, *J. Am. Chem. Soc.* **15**, 10286 (1993).
21. A. Mahammed, M. Rabinovitz, I. Willner, E. Vogel and M. Pohl, *J. Phys. Org. Chem.*, **8**, 658 (1995).
22. E. Vogel, M. Pohl, T. Wiss, C. König, J. Lex and M. Schmickler, in preparation.
23. H. A. Benesi and J. H. Hildebrand, *J. Am. Chem. Soc.* **71**, 2703 (1949).

## APPENDIX

The relationship between the concentration of the complex $A_2D$ and the absorption spectrum changes at the wavelength $\lambda$, $\Delta OD_\lambda$, equation (7), was derived by assuming that the absorbance at $\lambda$ is given by equation (A1). The formation of the complex obeys an $A_2D$ stoichiometry, equation (A2). The absorbance of A at wavelength $\lambda$ at an analytical concentration $[A]_0$ is $OD_\lambda^0$. As the experiment is performed by addition of an analytical concentration of the donor, $[D]_0$, to the measuring and reference cell, the absorbance change $\Delta OD_\lambda$ is given by equation (A3). As at wavelength $\lambda$ the electron acceptor absorbance is dominant ($\varepsilon_\lambda^A \gg \varepsilon_\lambda^D$, $\varepsilon_\lambda^{A_2D}$), equation (A3) can be expressed in terms of equation (A4), from which equation (7) is derived.

$$OD_\lambda = \sum \varepsilon_\lambda^i C_i \tag{A1}$$

$$2A + D \rightleftharpoons A_2D \tag{A2}$$

$$\Delta OD_\lambda = (OD_\lambda^0 - OD_\lambda) = (\varepsilon_\lambda^{A_2D} - \varepsilon_\lambda^D - 2\varepsilon_\lambda^A)[A_2D] \tag{A3}$$

$$\Delta OD_\lambda = -2\varepsilon_\lambda^A[A_2D] \tag{A4}$$

The rate expression for the formation of the complex $A_2D$, equation (6), is derived by solving the basic rate expression, equation (A5), where [A], [D] and $[A_2D]$ represent the concentrations of the electron acceptor, donor, and complex, respectively, at any time interval $t$. As [A] and [D] are given by equations (A6) and (A7), equation (A5) is transformed into equation (A8). The solution of this differential equation is given by equation (9), where the constant $C$, calculated for $t = 0$ and $[A_2D] = 0$, is expressed by equation (A10).

$$\frac{d[A_2D]}{dt} = k_2[A]^2[D] \tag{A5}$$

$$[A] = [A]_0 - 2[A_2D] \tag{A6}$$

$$[D] = [D]_0 - [A_2D] \tag{A7}$$

$$\frac{d[A_2D]}{([A]_0 - 2[A_2D]^2)([D]_0 - [A_2D])} = k_2\,dt \tag{A8}$$

$$\frac{1}{[A]_0 - 2[D]_0} \ln \frac{[A]_0 - 2[A_2D]}{[D]_0 - [A_2D]} - \frac{1}{[A]_0 - 2[A_2D]} = k_1([A]_0 - 2[D]_0)\, t + C \quad \text{(A9)}$$

$$C = \frac{1}{[A]_0 - 2[D]_0} \ln \frac{[A]_0}{[D]_0} - \frac{1}{[A]_0} \quad \text{(A10)}$$